Complex dynamics in initially separated reaction-diffusion systems

S. Havlin [a,b], M. Araujo [a], Y. Lereah [c], H. Larralde [a], A. Shehter [b], H.E. Stanley [a], P. Trunfio [a], B. Vilensky [b]

[a] *Center for Polymer Studies & Physics Department, Boston University, Boston, MA 02215, USA*
[b] *Department of Physics, Bar-Ilan University, Ramat-Gan, Israel*
[c] *Faculty of Engineering and Exact Sciences, Tel Aviv University, Tel Aviv 69978, Israel*

Abstract

We review recent developments in the study of the diffusion reaction systems of the type $A + B \rightarrow C$ in which the reactants are initially separated. We consider the case where the A and B particles are initially placed uniformly in Euclidean space at $x > 0$ and $x < 0$, respectively. We find that whereas for $d \geqslant 2$ the mean field exponent characterizes the width of the reaction zone, fluctuations are relevant in the one-dimensional system. We present analytical and numerical results for the reaction rate on fractals and percolation systems at criticality. We also study the case where the particles are Lévy flights in $d = 1$. Finally, we consider experimentally, analytically, and numerically the reaction $A + B_{\text{static}} \rightarrow C$, where species A diffuses from a localized source.

1. Introduction

The dynamics of diffusion controlled reactions of the type $A+B \rightarrow C$ has been studied extensively since the pioneering work of Smoluchowski [1,2]. Most studies have focused on homogeneous systems, i.e. when both reactants are initially uniformly mixed in a d-dimensional space, and interesting theoretical results have been obtained. When the concentrations of the A and B reactants are initially equal, i.e. $c_A(0) = c_B(0) = c(0)$, the concentration of both species is found to decay with time as, $c(t) \sim t^{-d/4}$ for Euclidean $d \leqslant 4$ dimensional systems [3–10] and as $c(t) \sim t^{-d_s/4}$ for fractals [5,6] with fracton dimension $d_s \leqslant 2$. Also, self-segregated regions of A and B in low dimensions ($d \leqslant 3$) [4] and in fractals [9] have been found. Quantities such as the distributions of domain sizes of segregated regions and interparticle distances between species of the same type and different types have been calculated [11–13]. These systems were also studied theoretically and numerically under steady state conditions and several interesting

predictions have been obtained [14–17]. However, the above numerical and theoretical predictions have not been observed in experiments, in part because of difficulties to implement the initially uniformly-mixed distribution of reactants.

In recent years it was realized that diffusion reaction systems in which the reactants are initially separated [18] can be studied experimentally [19,20] and that the dynamics of such a system have many surprising features [20–27]. These systems are characterized by the presence of a dynamical interface or a front that separates the reactants. Such a reaction front appears in many biological, chemical and physical processes [28–34].

Gàlfi and Ràcz [18] studied the diffusion-controlled reaction system with initially separated reactants. They studied the kinetics of the reaction diffusion process using a set of mean-field (MF) type equations,

$$\frac{\partial c_A}{\partial t} = D_A \frac{\partial^2 c_A}{\partial x^2} - k c_A c_B , \tag{1a}$$

$$\frac{\partial c_B}{\partial t} = D_B \frac{\partial^2 c_B}{\partial x^2} - k c_A c_B. \tag{1b}$$

Here $c_A \equiv c_A(x,t)$ and $c_B \equiv c_B(x,t)$ are the concentrations of A and B particles at position x at time t respectively, $D_{A,B}$ are the diffusion constants and k is the reaction constant. The rate of production of the C-particles at site x and time t, which we call the reaction-front profile, is given by $R(x,t) \equiv k c_A c_B$. The initial conditions are that the A species are uniformly distributed on the right-hand side of $x = 0$ and the B species are uniformly distributed on the left-hand side.

Using scaling arguments, Gàlfi and Ràcz [18] find that the width w of the reaction front $R(x,t)$ scales with time as, $w \sim t^\alpha$ with $\alpha = 1/6$ and the reaction rate at the center of the front, which is called the reaction height, scales as $h \sim t^{-\beta}$ with $\beta = 2/3$.

Experiments [19] and simulations [19,21–24] for $d \geqslant 2$ systems in which both reactants diffuse, support the above predicted values for α and β. Indeed, Cornell et al. [23] argue that the upper critical dimension is $d = 2$ and the MF approach should therefore be valid for $d \geqslant 2$. Moreover, numerical simulations of 1D systems show that the width exponent appears to be $\alpha \simeq 0.3$ and the height exponent $\beta \simeq 0.8$ [23,24]. Recently [25] it was argued that α varies between 1/4 and 3/8, depending on the moment at which the width is calculated. For controversial discussions about the existence of multiscaling, see Refs. [35–39]. The origin of the difference between the exponents of 1D systems and those of higher dimensional systems is due to fluctuations in the location of the front which are important in low dimensions and are neglected in the MF approach.

Taitelbaum et al. [20,22] studied analytically Eqs. (1) and presented experiments for the limit of small reaction constant or short time. The main results are that several measurable quantities undergo interesting crossovers. For example, the global reaction rate changes from $t^{1/2}$ in the short time limit to $t^{-1/2}$ at the asymptotic time regime. The center of the front can change its direction of motion as found in experiments [20]. Ben-Naim and Redner [26] studied the solution of (1) under steady-state conditions. A persistence model of Eq. (1) was recently studied by Vilensky et al. [40].
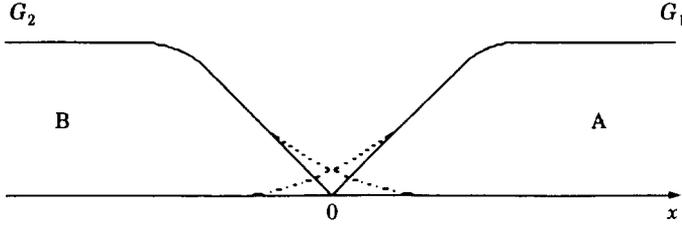
Fig. 1. Schematic picture of the reactant concentration profiles near the origin. The solid lines represent the $G_{1,2}(x,t)$ part of the profile, the dashed lines represent the complete form $G_{1,2}(x,t) \pm \delta c(x,t)$. Note that the profile of species A is given solely by $\delta c(x,t)$ on the left of the origin. (From Ref. [27].)

2. The form of the reaction front, $R(x,t)$, in the mean-field approach

In a recent work [27], we consider the symmetric case in which both diffusion constants and initial concentrations are equal, i.e. $D_A = D_B \equiv D$ and $c_A(x,0) = c_B(x,0) = c_0$. If we define $F(x,t) \equiv c_A(x,t) - c_B(x,t)$, then from Eq. (1) follows

$$\frac{\partial F}{\partial t} = D \frac{\partial^2 F}{\partial x^2}, \tag{2}$$

subject to the conditions that initially the A particles are uniformly distributed to the right of the origin while the B particles are uniformly distributed to the left of the origin. Eq. (2) has the solution $F(x,t) = c_0 \, \mathrm{erf}(x/\sqrt{4Dt})$.

We rewrite the concentrations of A and B particles as (see Fig. 1)

$$c_A(x,t) = G_1(x,t) + \delta c_1(x,t), \qquad c_B(x,t) = G_2(x,t) + \delta c_2(x,t), \tag{3}$$

where

$$G_1(x,t) = \begin{cases} F(x,t) & [x > 0], \\ 0 & [x < 0], \end{cases} \tag{4}$$

and $G_2(x,t) = G_1(-x,t)$. It is easy to see that under the above conditions, $\delta c_1(x,t) = \delta c_2(x,t) \equiv \delta c(x,t)$. Substituting Eqs. (3) into Eqs. (1) yields

$$\frac{\partial(\delta c)}{\partial t} = D \frac{\partial^2(\delta c)}{\partial x^2} - k \left(c_0 \, \mathrm{erf} \left(\frac{x}{\sqrt{4Dt}} \right) + \delta c \right) \delta c. \tag{5}$$

The asymptotic solution for this equation that vanishes as $x \to \infty$ is

$$\delta c(x,t) \sim t^{-1/3} \left(\frac{x}{t^{1/6}} \right)^{-1/4} \exp \left[-\frac{2}{3} \left(\frac{\lambda x}{t^{1/6}} \right)^{3/2} \right], \quad t^{1/6} \ll x \ll (4Dt)^{1/2}, \tag{6}$$

where $\lambda = (ka/D)^{1/3}$, $a \equiv c_0/(\pi D)^{1/2}$. As may be confirmed by direct substitution, this expression is a solution of Eq. (5) up to terms of order $(\delta c)/t$, which can be neglected for large t.

Using Eq. (6) we can write an expression for the reaction-front profile $R(x,t)$ defined in (1) as

$$R(x,t) \simeq \frac{kax}{t^{1/2}}(\delta c) \sim t^{-2/3}\left(\frac{x}{t^{1/6}}\right)^{3/4}\exp\left[-\frac{2}{3}\left(\frac{\lambda x}{t^{1/6}}\right)^{3/2}\right]. \tag{7}$$

It is seen that the width of the reaction front grows as $t^{1/6}$, whereas the height can be identified with the prefactor $t^{-2/3}$ in Eq. (7), consistent with the exponents found by Gàlfi and Ràcz [18]. Eq. (7) provides a more quantitative solution of Eqs. (1) than the previous scaling arguments [18], as well as information on the dependence of the form of the reaction front on the parameters c_0, k, and D, for the symmetric case.

For the case in which one reactant is static no analytical solution (of Eq. (1)) exists for the form of the reaction-front profile. However, numerical solutions of Eq. (1) with $D_B = 0$ shown in Fig. 2, suggest that $R(x',t) \sim t^{-\beta}g(x'/t^{\alpha})\exp(-|x'|/t^{\alpha})$, where $x' \equiv x - \gamma t^{1/2}$. The excellent scaling in Fig. 2b suggests that the width does not increase with time, i.e. $w \sim t^{\alpha}$ with $\alpha = 0$ and $h \sim t^{-\beta}$ with $\beta = 1/2$, consistent with the scaling arguments in Ref. [21].

3. The front $R(x,t)$ in $d = 1$

The reaction-front profile in $d = 1$ systems, $R(x,t)$, when both reactants are diffusing with the same diffusion constant, $D_A = D_B \neq 0$, has been calculated numerically [24]. The data shown in Fig. 3 suggests that

$$c_C(x,t) \equiv \int_0^t R(x,t')dt' \sim \exp(-a|x|/t^{\alpha}), \tag{8}$$

with $\alpha = 0.33 \pm 0.05$.

For the case $D_A \neq 0$, $D_B = 0$, analytical and numerical studies [41] yield for the reaction-front profile

$$R(x,t) = \frac{1}{4t^{3/4}}\left(\frac{2\gamma^2}{\mu\pi}\right)^{1/2}\exp\left(-\frac{(x-\gamma t^{1/2})^2}{2\mu t^{1/2}}\right)\left(1 + \frac{x-\gamma t^{1/2}}{2\gamma t^{1/2}}\right), \tag{9}$$

where γ and μ are constants. From Eq. (9) it follows that $\alpha = 1/4$ and $\beta = 3/4$. It is interesting to note that the time integral of $R(x,t)$, which is the total production of the C particles at x up to time t, is given by

$$c_C(x,t) = \int_0^t R(x,\tau)d\tau = \frac{1}{2}\text{erfc}\left(\frac{x-\gamma t^{1/2}}{\sqrt{2\mu t^{1/2}}}\right). \tag{10}$$

To summarize the case of $A + B \rightarrow C$ with initially separated reactants, we list in Table 1 the four sets of exponents discussed above.
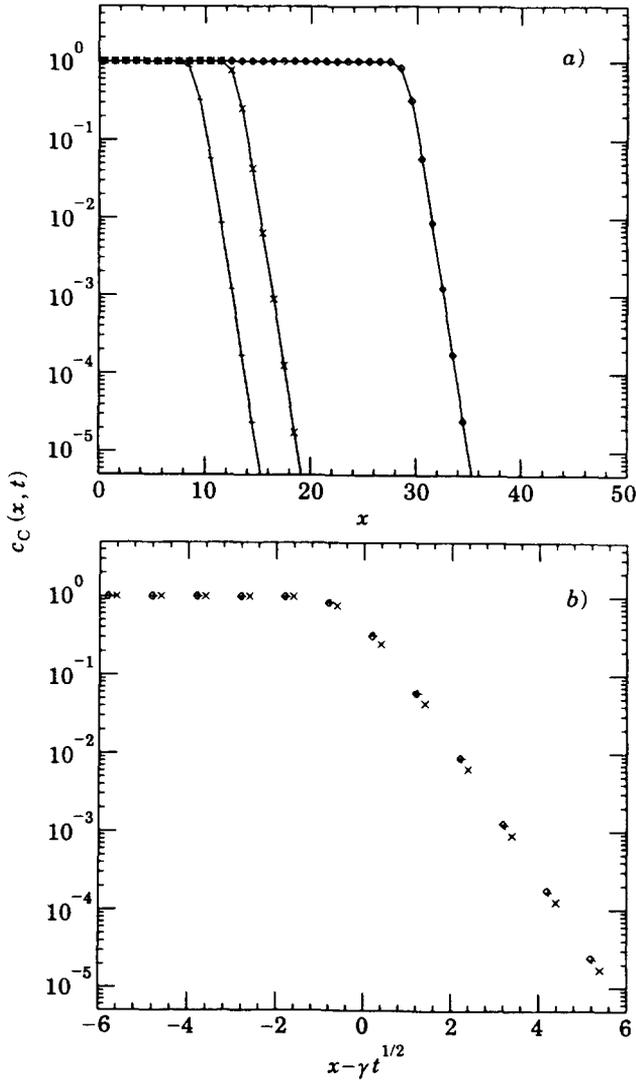
Fig. 2. Numerical solution of Eq. (1) for the case $D_B = 0, D_A \neq 0$: (a) plot of $c(x,t)$ as a function of x for $t = 500, 1000$ and 5000; (b) the scaling plot of $c(x,t)$ as a function of $(x - \langle x \rangle)$ indicates that $\alpha = 0$ and $\beta = 1/2$.

4. The reaction rate on percolation clusters

The case of $A + B \rightarrow C$ with initially separated reactants on fractal systems was studied on the $d = 2$ infinite percolation cluster at criticality [22]; for a demonstration of the system see Fig. 4. It is expected that the total number of reactants up to time t, scales as the mean displacement of a random walker on a fractal, i.e.
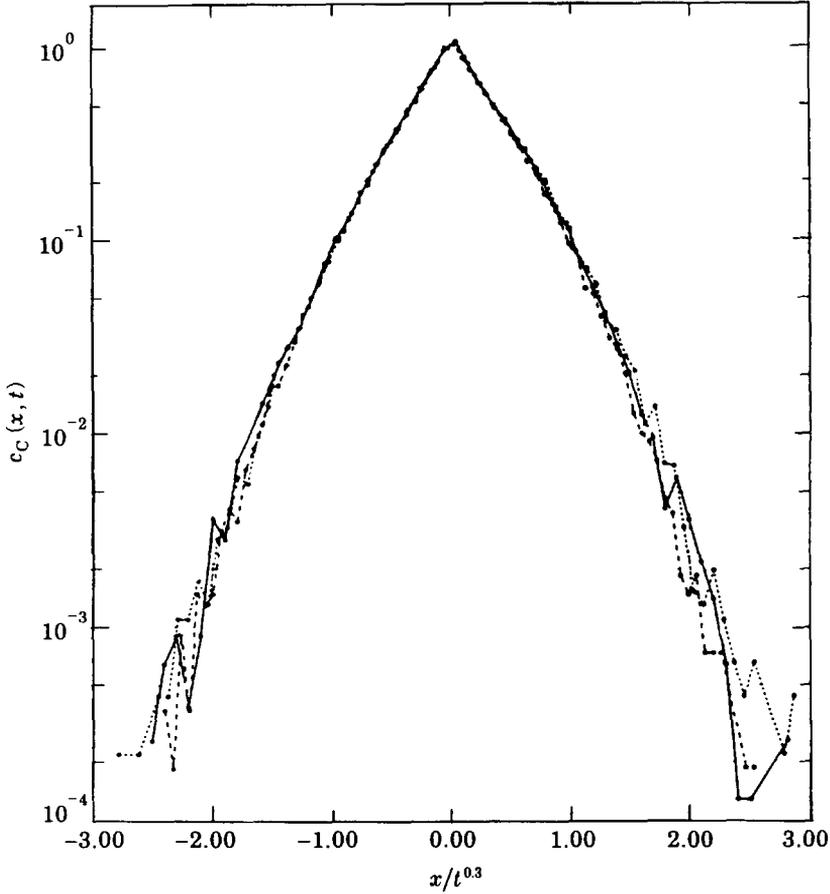
Fig. 3. Plot of $c_C(x,t)$ defined in Eq. (8) for $d = 1$ system with system size $L = 10\,000$ and $t = 1000, 5000$ and $10\,000$.

Table 1
The values of the exponents α and β ($w \sim t^{\alpha}$, $h \sim t^{-\beta}$)

	$d = 1$	MF
Both moving	$\alpha \cong 0.3$	$\alpha = 1/6$
	$\beta \cong 0.8$	$\beta = 2/3$
One static	$\alpha = 1/4$	$\alpha = 0$
	$\beta = 3/4$	$\beta = 1/2$

$$\int_0^t R(t')\,dt' \sim \langle r^2 \rangle^{1/2} \sim t^{1/d_w},$$

where d_w is the anomalous diffusion exponent [42]. From this it follows that the reaction rate

$$R(t) \equiv \int_{-\infty}^{\infty} R(x,t)dx \sim t^{-\gamma}, \qquad \gamma = 1 - 1/d_w. \tag{11}$$

One must distinguish between reaction diffusion on the infinite cluster and on the percolation system, containing also small clusters [43]. The reaction rate on the infinite cluster is smaller and decrease slower compared with the system containing clusters of all sizes. This can be understood as follows.

Applying scaling arguments we can say that up to time t the reaction invades a typical length $r^* \sim t^{1/d_w}$ which corresponds to the cluster mass $s^* \sim r^{*d_f} \sim t^{d_f/d_w}$. Thus, at any finite time t we can divide all clusters into two groups according to their sizes: *active* clusters of mass $s > s^*$, in which particles are not aware of the finiteness of their cluster (this group contains the infinite cluster), and *inactive* clusters of mass $s < s^*$ on which at least one of the reactants has vanished and the reaction rate is zero. According to this picture, in the full percolation system, which contains clusters of all sizes, at any time there are active clusters of finite size that can contribute to the reaction rate. Therefore, the rate of reaction in the percolation system is always higher than the rate on the infinite cluster alone. Moreover, since s^* is growing with time there are always some clusters that become inactive, causing an additional (apart from the one caused by slowing of the diffusion rate on the infinite cluster network) decrease of the rate of reaction in the percolation system. Since the system is self-similar this has to influence the reaction rate exponent.

To make the quantitative description of the above considerations we will look on each cluster of mass s and linear size $r \sim s^{1/d_f}$ as a reservoir of particles divided by the *front line* into A and B parts. The sites of a given cluster lying on a front line form, which we call an *active front*. The length ℓ_s of the active front in a cluster of mass s is expected to be

$$\ell_s \sim r^{d_f-1} \sim s^{(d_f-1)/d_f}. \tag{12}$$

Next we assume that rate of reaction on a cluster per unit length of active front is

$$R_0(t) \sim \begin{cases} t^{-\gamma}, & t < t^*, \\ 0, & t > t^*, \end{cases} \tag{13}$$

where $t^* = s^{d_w/d_f}$. Therefore, the total contribution of all the active clusters of size s to the reaction rate is

$$R_s(t) \sim \varphi_s s^{(d_f-1)/d_f} t^{-\gamma}, \tag{14}$$

where φ_s is number of clusters of size s that intersect the front line. One can estimate φ_s as follows. In a percolation system of size $L \times L$ there are n_s clusters of mass s. Only a small part of them intersects the front line, namely those in a strip of width $w \sim s^{1/d_f}$ around the front line. Their fraction is w/L. Therefore, $\varphi_s \sim (s^{1/d_f}/L)n_s \sim s^{1/d_f}n_s$. Substituting this in (14) we get

$$R_s(t) \sim s^{1/d_f} n_s s^{(d_f-1)/d_f} t^{-\gamma} = t^{-\gamma} s n_s. \tag{15}$$

Fig. 4.
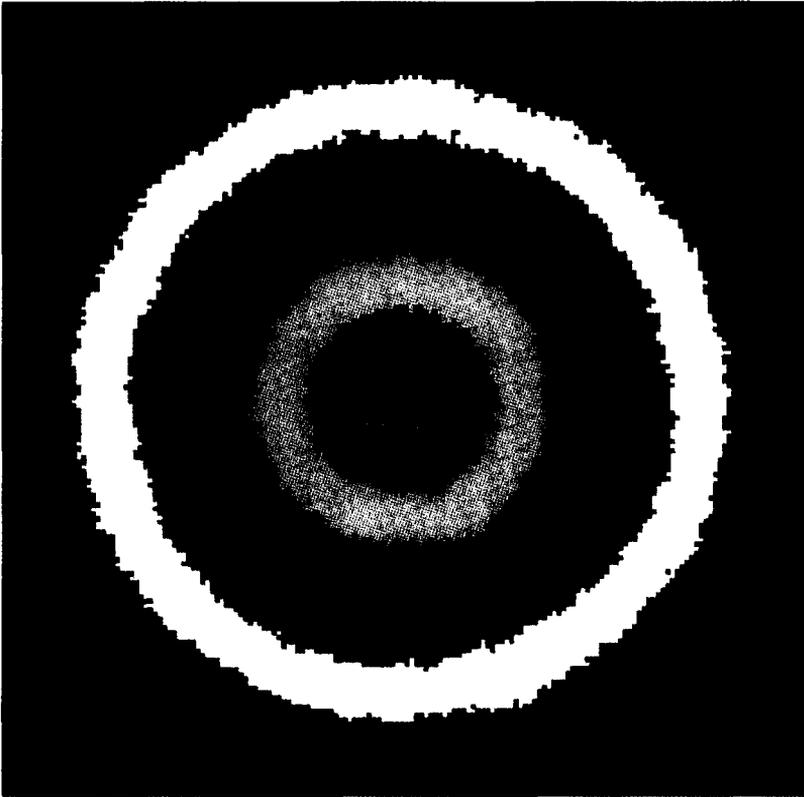

Fig. 8.

Thus, the reaction rate in the percolation system is

$$R(t) = \sum_{s=s^*}^{\infty} R_s(t) = t^{-\gamma}(s^*)^{2-\tau} = t^{-\gamma}t^{-\delta} = t^{-\gamma'},$$

$$\delta = \gamma' - \gamma = \frac{d_f}{d_w}(\tau - 2). \tag{16}$$

Hence, the effect of the dying clusters changes the reaction rate exponent, as expected. These results are in good agreement with our numerical simulations, see Fig. 5.

We also study the finite size effects on the reaction diffusion system. For a percolation system of size $L \times L$ we expect that for the infinite cluster,

$$R(t) = L^{d_f - 1}t^{-\gamma}, \tag{17a}$$

while for the percolation system

$$R(t) = Lt^{-\gamma'}. \tag{17b}$$

We expect that at time $t^* \sim L^{d_w}$ these two rates become equal, since no "small" active cluster exist in the system above t^*. Indeed, equating the last two expressions of (17) reproduces Eq. (16). The prefactor L in (17b) assures that the reaction rate for percolation system is larger for $t < t^*$ than the reaction rate on the infinite cluster. Indeed, the ratio of the reaction rates at $t = 1$ is L^{2-d_f}.

5. The reaction front of Lévy flights in $d = 1$

The initially separated reaction $A + B \rightarrow C$, where the particles have Lévy flight properties have been studied on the $d = 1$ Euclidean system [44]. The average displacement for a Lévy flight is $\langle |x| \rangle \propto t^{1/\gamma}$, where $1 < \gamma \leqslant 2$ [45]. So the reaction rate scales with time as

$$R(t) = \int_{-\infty}^{\infty} R(x,t)dx \sim t^{1/\gamma - 1}. \tag{18}$$

Applying scaling arguments on the mean field (MF) set of Eqs. (1), we find that the width w of the reaction front $R(x,t)$ scales with time as $w \sim t^{\alpha}$ with

Fig. 4. Reaction-diffusion on the two-dimensional infinite percolation cluster at criticality at $t = 2000$. White squares represent sites of the infinite cluster. Blue and red circles represent the A and B particles. Initially all sites of cluster in the right half plane and left half plane were occupied by A and B particles, respectively.

Fig. 8. Numerical simulations of $A + B_{static} \rightarrow C_{inert}$ where A particles are injected at rate $\lambda = 5$ at the center of the lattice and particles of type B are static and are located at each site of a $d = 2$ lattice. Plot of the reactant area after $t = 20, 160, 540, 1280, 2500, 4320$ and 6860.
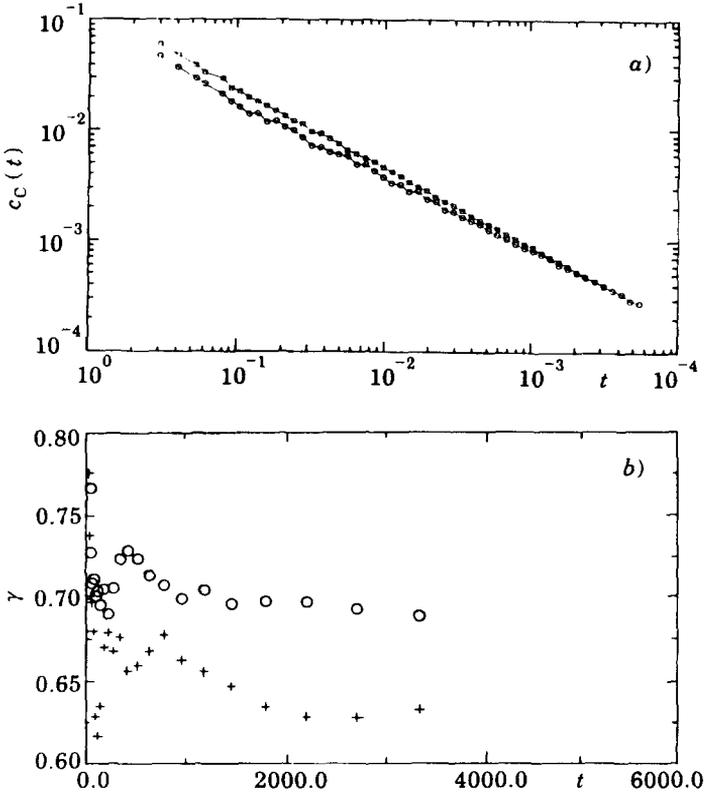
Fig. 5. (a) Plot of the rate $c_C(t)$ for the percolation system ($\diamond$) and for the infinite percolation cluster ($\circ$). (b) Plot of successive slopes of the data in (a). The exponent γ of reaction rate on the infinite cluster (+) and on the percolation system ($\circ$).

$$\alpha = 1/\gamma - 1/3, \tag{19a}$$

and the reaction height, scales as $h \sim t^{-\beta}$ with

$$\beta = 2/3, \tag{19b}$$

independent of γ. The value of $\gamma = 2$ is critical value above which regular diffusion exists. In Fig. 6, we compare our numerical simulations with the prediction of Eqs. (19).

6. The reaction rate $A + B_{\text{static}} \rightarrow C_{\text{inert}}$: Localized source of A

Another system in which the reactants are initially separated and which is amenable to experiment, is the reaction $A + B_{\text{static}} \rightarrow C_{\text{inert}}$ with a localized source of A species. There exist many systems in nature in which a reactant A is "injected" into a d-dimensional substrate B where upon it reacts to form an inert product C. Recently such
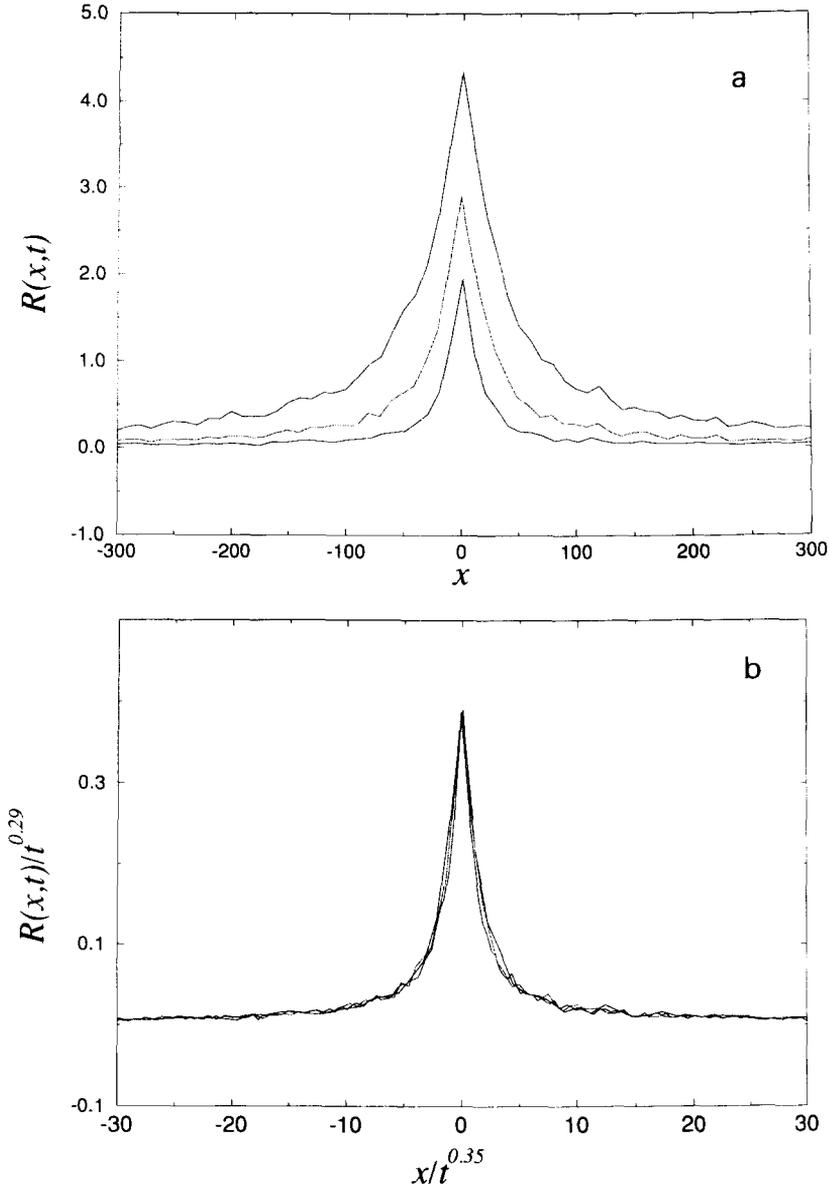
Fig. 6. (a) The integral of the reaction profile $\tilde{R}(x,t) = \int_0^t R(x,t')dt'$ for the reaction $A + B \rightarrow C$ where A and B are Levy flights with $\gamma = 1.5$ at t=256 (lower curve), t=1024 (middle curve) and t=4096 (upper curve). (b) The scaling of the data presented in (a). Note that the MF predictions are $\beta=2/3$ and $\alpha=1/3$ compared to $\beta \simeq 0.71$ and $\alpha \simeq 0.4$ obtained in simulations.

an experiment has been performed [46] by injecting iodine at a point of a large silver plate and measuring quantities of the reaction $I_{2\ gas} + 2Ag_{solid} \rightarrow 2AgI_{solid}$.

First we consider N particles of type A that are initially at the origin of a lattice. The B particles are static and distributed uniformly on the lattice sites. Using an approximate
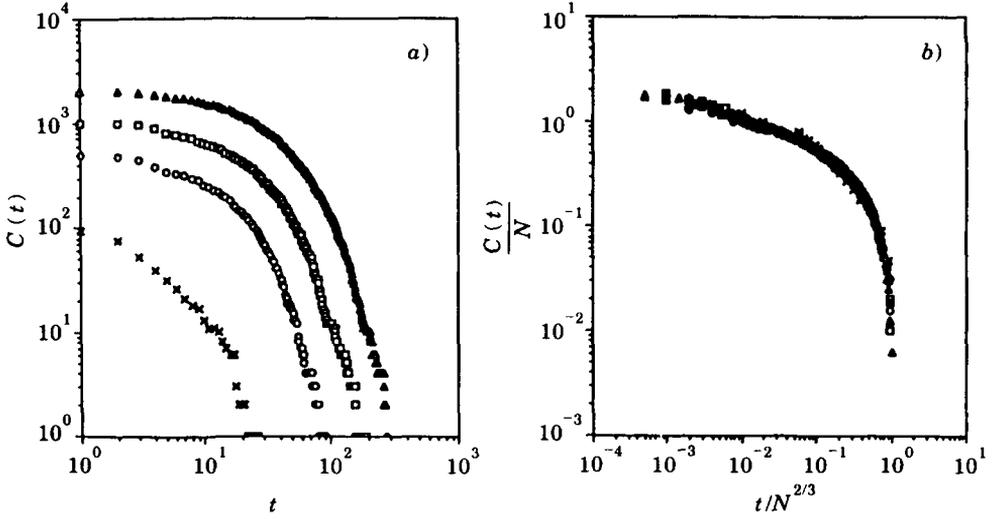
Fig. 7. Numerical simulations of $A + B \rightarrow C$ where N diffusing particles of type A are initially at the center of a lattice and particles of type B are static and located at each site of the $d = 3$ lattice: (a) plot of $C(t)$ for $N = 100$ ($\times$), 500 ($\bullet$), 1000 ($\square$), and 2000 ($\triangle$) particles; (b) plot of $C(t)$ in the scaling form Eq. (24a). Note that the results are of a *single* Monte Carlo run and not averaged—showing that fluctuations are negligible in this process.

quasi-static [47] analytical approach for trapping in a moving boundary we derived expressions for $C(t)$, the time-dependent growth size of the C region and for $S(t)$ the number of surviving A particles at time t. For extremely short time $t < t_\times \sim \ln N$ we find $C(t) \sim t^d$. For $t > t_\times$ we find [48]

$$C(t) \sim Nf\left(\frac{t}{N^{2/d}}\right) \qquad \text{and} \qquad S(t) = N - C(t). \tag{20a}$$

The scaling function $f(u)$ is the solution to the differential equation

$$\frac{df}{d\tau} \sim k_d f^{-2/d}[1 - f], \tag{20b}$$

and k_d is a constant, depending only on dimension. Fig. 7 shows simulation data supporting (20a).

Now consider the case in which λ particles of type A are injected per unit time at the origin of the lattice. For this case we find [46]

$$C(t) \sim \begin{cases} \sqrt{8Dt \ln(\lambda^2 t/2D)}, & d = 1, \\ \pi\alpha t, & d = 2, \\ \lambda t, & d = 3, \end{cases} \tag{21}$$

and

$$S(t) \sim \begin{cases} \lambda t, & d = 1, \\ (\lambda - \pi\alpha)t, & d = 2, \\ C_3(\lambda)t^{2/3}, & d = 3. \end{cases} \tag{22}$$

In (21) and (22), α is the solution of $\alpha\pi = \lambda\, e^{-\alpha/4D}$ and $C_3(\lambda) = (\lambda/4D)(3\lambda/4\pi)^{2/3}$. Moreover, we find that for both one- and three-dimensional systems $C(t)$ satisfies the scaling relation

$$C(t) \sim \lambda^{d/(d-2)} g\left(\frac{t}{\lambda^{2/(d-2)}}\right). \tag{23}$$

Eqs. (21) and (22) have been supported by numerical simulations [46]. (See also Fig. 8.) Eqs. (20) can be generalized for fractals:

$$C(t) \sim N f\left(\frac{t}{N^{2/d_s}}\right), \tag{24a}$$

where $f(u)$ is the solution of the differential equation

$$\frac{df}{du} \sim k_{d_s} f^{-2/d_s}[1 - f]. \tag{24b}$$

Here d_s is the fracton dimension defined by $d_s = 2d_f/d_w$, in which d_f is the fractal dimension and d_w the diffusion exponent [49]. For the case of constant injection rate on a fractal we do not have an analytical derivation. However, we recently calculated [50] the number of distinct sites visited on a fractal by N random walkers starting from the origin, $S_N(t) \sim (\ln N)^{d_f/\delta} t^{d_s/2}$ with $\delta = d_w/(d_w - 1)$. This result can be shown to be valid also for the number of distinct site visited by random walkers injected at the origin with a constant rate λ when replacing $N = \lambda t$. Thus we obtain that $(\ln \lambda t)^{d_f/\delta} t^{d_s/2}$ is an upper bound for $C(t)$.

Acknowledgements

References

[1] M. V. Smoluchowski, Z. Phys. Chem. 92 (1917) 129.
[2] See, e.g., S.A. Rice, Diffusion-Limited Reactions (Elsevier, Amsterdam, 1985).
[3] A. A. Ovchinnikov and Y.B. Zeldovich, Chem. Phys. 28 (1978) 215.
[4] D. Toussiant and F. Wilzeck, J. Chem. Phys. 78 (1983) 2642.
[5] P. Meakin and H.E. Stanley, J. Phys. A 17 (1984) L173.
[6] K. Kang and S. Redner, Phys. Rev. Lett. 52 (1984) 955; Phys. Rev. A 32 (1985) 435.
[7] K. Lee and E.J. Weinberg, Nucl. Phys. B 246 (1984) 354.
[8] G. Zumofen, A. Blumen and J. Klafter, J. Chem. Phys. 82 (1985) 3198.
[9] R. Kopelman, Science 241 (1988) 1620.
[10] M. Bramson and J.L. Lebowitz, Phys. Rev. Lett. 61 (1988) 2397; J. Stat. Phys. 65 (1991) 941.
[11] P. Argyrakis and R. Kopelman, Phys. Rev. A 41 (1990) 2121.
[12] G.H. Weiss, R. Kopelman and S. Havlin, Phys. Rev. A 38 (1989) 466.
[13] F. Leyvraz and S. Redner, Phys. Rev. Lett. 66 (1991) 2168;
      S. Redner and F. Leyvraz, J. Stat. Phys. 65 (1991) 1043.
[14] L.W. Anacker and R. Kopelman, Phys. Rev. Lett. 58 (1987) 289; J. Chem. Phys. 91 (1987) 5555.

[15] K. Lindenberg, B.J. West and R. Kopelman, Phys. Rev. Lett. 60 (1988) 1777.

[16] D. ben-Avraham and C.R. Doering, Phys. Rev. A 37 (1988) 5007.

[17] E. Clément, L.M. Sander and R. Kopelman, Phys. Rev. A 39 (1989) 6455.

[18] L. Gálfi and Z. Rácz, Phys. Rev. A 38 (1988) 3151.

[19] Y.E. Koo, L. Li and R. Kopelman, Mol. Cryst. Liq. Cryst. 183 (1990) 187;
Y.E. Koo and R. Kopelman, J. Stat. Phys. 65 (1991) 893.

[20] H. Taitelbaum, Y.E. Koo, S. Havlin, R. Kopelman and G.H. Weiss, Phys. Rev. A 46 (1992) 2151.

[21] Z. Jiang and C. Ebner, Phys. Rev. A 42 (1990) 7483. .

[22] H. Taitelbaum, S. Havlin, J. Kiefer, B.L. Trus and G.H. Weiss, J. Stat. Phys. 65 (1991) 873.

[23] S. Cornell, M. Droz and B. Chopard, Phys. Rev. A 44 (1991) 4826.

[24] M. Araujo, S. Havlin, H. Larralde and H.E. Stanley, Phys. Rev. Lett. 68 (1992) 1791.

[25] M. Araujo, H. Larralde, S. Havlin and H.E. Stanley, Phys. Rev. Lett. 71 (1993) 3592.

[26] E. Ben-Naim and S. Redner, J. Phys. A 25 (1992) L575.

[27] H. Larralde, M. Araujo, S. Havlin and H.E. Stanley, Phys. Rev. A 46 (1992) 855.

[28] D. Avnir and M. Kagan, Nature 307 (1984) 717.

[29] G.T. Dee, Phys. Rev. Lett. 57 (1986) 275.

[30] B. Heidel, C.M. Knobler, R. Hilfer and R. Bruinsma, Phys. Rev. Lett. 60 (1986) 2492.

[31] R.E. Liesegang, Naturwiss. Wochensch. 11 (1896) 353.

[32] T. Witten and L.M. Sander, Phys. Rev. Lett. 47 (1981) 1400.

[33] R.A. Ball, Ausr. Gemmol. 12 (1984) 89.

[34] K.F. Mueller, Science 255 (1984) 1021.

[35] S. Cornell, Phys. Rev. Lett. 75 (1995); Phys. Rev. 51 (1995) 4055.

[36] M. Araujo, H. Larralde, S. Havlin and H.E. Stanley, Phys. Rev. Lett. 75 (1995).

[37] A. Rodriguez and H.S. Wio, in press.

[38] M. Howard and J. Cardy, J. Phys. A (1995), in press.

[39] B.P. Lee and J. Cardy, Phys. Rev. E 50 (1994) R3287.

[40] B. Vilensky, S. Havlin, H. Taitelbaum and G.H. Weiss, J. Phys. Chem. 98 (1994) 7325.

[41] H. Larralde, M. Araujo, S. Havlin and H.E. Stanley, Phys. Rev. A 46 (1992) R6121.

[42] A. Bunde and S. Havlin, eds., Fractals and Disordered Systems (Springer, Heidelberg, 1991); Fractals in Science (Springer, Heidelberg, 1994);
G.H. Weiss, Aspects and Applications of the Random Walk (North-Holland, Amsterdam, 1994);
A.-L. Barabasi and H.E. Stanley, Fractal Concepts in Surface Growth (Cambridge University Press, Cambridge, 1995).

[43] S. Havlin and D. Ben-Avraham, Adv. Phys. 36 (1987) 695.

[44] M.F. Shlesinger, G. Zaslavsky and J. Klafter, Nature 263 (1993) 31; Levy Flights and Processes, eds. M.F. Shlesinger, G. Zaslavsky and U. Frisch (Springer, Berlin, 1995);
M.F. Shlesinger and J. Klafter, Phys. Today (in press).

[45] B. Vilensky and S. Havlin (preprint).

[46] H. Larralde, Y. Lereah, P. Trunfio, J. Dror, S. Havlin, R. Rosenbaum and H.E. Stanley, Phys. Rev. Lett. 70 (1993) 1461.

[47] J. Crank, Free and Moving Boundary Problems (Clarendon Press, Oxford, 1984).

[48] H. Larralde, P. Trunfio, S. Havlin and H.E. Stanley, preprint.

[49] S. Alexander and R. Orbach, J. Physique Lett. 43 (1987) L625.

[50] H. Larralde, P. Trunfio, S. Havlin, H.E. Stanley and G.H. Weiss, Nature 355 (1992) 423; Phys. Rev. A 45 (1992) 7128;
S. Havlin, H. Larralde, P. Trunfio, J.E. Kiefer, H.E. Stanley and G.H. Weiss, Phys. Rev. A 46 (1992) R-1717.